Theoretical Study of the Low-Lying Electronically Excited States of OBrO

Reinhard Vetter,* Thomas Ritschel, and Lutz Zülicke

Institut für Chemie, Universität Potsdam, Postfach 60 15 53, D-14415 Potsdam, Germany

Kirk A. Peterson

Department of Chemistry, Washington State University, Pullman, Washington 99164 and The William R. Wiley Environmental Molecular Sciences Laboratory, Pacific Northwest National Laboratory, Richland, Washington 99352

Received: August 23, 2002

Motivated by the possible importance of OBrO in atmospheric photochemistry, multireference configuration interaction calculations of the low-lying excited states were carried out to obtain information about the electronic vertical spectrum up to excitation energies of about 6 eV from the ground state, including the transition dipole moments, and about possible photodissociation pathways, based on one-dimensional cuts through the potential energy surfaces for dissociation into BrO + O and Br + O_2, respectively. In addition, for probing the angle dependence the bending potentials were also calculated. From all computed eight doublet states (two/four of each symmetry in C_{2v} C_s) only the 1^2A_2 state at 2.7 eV possesses a large transition dipole moment with the 1^2B_1 ground state, whereas for all other states this quantity is very small or zero. Therefore the 1^2A_2 state should play a decisive role in OBrO photochemistry. Close to the 1^2A_2 state two other states were found at 2.4 eV (1^2B_2) and 2.5 eV (1^2A_1) so that interactions of these three states should certainly influence possible dissociation processes. For this reason, besides direct adiabatic photodissociation of the 1^2A_2 state into BrO + O also predissociation via these close-lying states can be expected, leading to a very complex photodissociation mechanism for excitation energies around 2.5 eV. Moreover, in this energy range photodissociation into Br + O_2 is only possible through the 1^2B_2 state (after initial excitation of the 1^2A_2 state) because only for this state a small barrier of 0.7 eV relative to its minimum is estimated from the calculation of a simplified C_{2v} minimum energy path. For the 1^2A_1 and 1^2A_2 states, rather large barriers are predicted. The next higher-lying states, with excitation energies of 3.9 eV (2^2A_1) and 4.5 eV (2^2B_2) are well separated from lower- and higher-lying states and from each other, but due to their small transition dipole moments, they should be probably of minor importance for the OBrO photochemistry. The last two states considered in our study are predicted to lie close together at 6.0 eV (2^2A_2) and 6.1 eV (2^2B_1) and are strongly repulsive upon dissociation into BrO + O. Finally, it should be noted that our calculations demonstrate the expected qualitative similarity to the results previously obtained for the corresponding OClO system.

Introduction

It has become highly probable in the past decade that in addition to chlorine, bromine oxides (especially BrO) also play an important role in catalytic cycles of stratospheric ozone destruction. This fact stimulated the detailed experimental and theoretical investigation of the properties and processes involving these species.[1] Up to the present time, the knowledge about bromine oxides is far from being complete, as can be clearly seen by comparison of the halogen dioxides OClO and OBrO. Contrary to OClO which is well characterized experimentally and theoretically,[2−5] much less is known about OBrO.[5,6] This is not unexpected, because the investigation of the OBrO radical turns out to be more difficult experimentally (very unstable system) as well as theoretically (electron-rich system). Moreover, the participation of OBrO in ozone destruction processes is presently still not quite clear, because spectroscopic observations in the stratosphere and model calculations gave contradictory results. Whereas balloon-borne spectroscopic investigations of Renard et al.[7] presumably detected OBrO in the stratosphere in significant quantities, model calculations performed by Chipperfield et al.[8] indicate much smaller abundances of this species. Recently, measurements of OBrO limits in the nighttime stratosphere by Erle et al.[9] suggest a negligible role of OBrO in stratospheric photochemistry as well. Thus, the importance of OBrO in atmospheric bromine chemistry remains uncertain and more information about the photochemistry of OBrO, especially photodissociation cross sections, is highly desirable.

At present, only a few experimental and theoretical studies dealing with the electronically excited states of OBrO are available, mainly limited to the characterization of the $1^2A_2(C^2A_2)$ state. The first visible spectrum of OBrO in the gas phase due to the $C^2A_2 \leftarrow X^2B_1$ electronic transition was reported by Rattigan et al.[10] Somewhat later, Miller et al.[11] reinvestigated the spectrum and made use of the results of quantum-chemical calculations for a reliable interpretation of the experimental findings. Furthermore, two studies of the electronic spectrum in rare gas matrices were also carried out.[12,13] Important for comparison with theoretical predictions is the first measurement of UV/vis absorption cross sections for gas-phase OBrO at room temperature by Knight et al.[14]

Finally, two theoretical papers dealing with electronically excited states of OBrO should be mentioned. In the first paper,

* Corresponding author. E-mail: vetter@tcb12.chem.uni-potsdam.de.

10.1021/jp021952p CCC: $25.00
Published on Web 02/08/2003

Miller et al.[11] carried out CCSD(T) calculations to determine the geometries and relative energies of the four lowest-lying states X^2B_1, A^2B_2, B^2A_1, and C^2A_2. In the second paper, Peterson[5] used the multireference configuration interaction method to calculate near-equilibrium potential energy functions (PEF) for the X^2B_1 and C^2A_2 states. On the basis of the PEF results the vibrational spectra were calculated.

Altogether, there is still relatively scarce information on this interesting and important system; because of that we started more comprehensive calculations of the low-lying excited states of OBrO with the final aim of predicting cross sections for the relevant photodissociation processes.

In a first step, we report in this paper about extensive CASSCF-MRCI calculations of the electronic vertical spectrum (eight doublet states and four quartet states) and the corresponding transition dipole moments from the X^2B_1 ground state. To get a first impression about possible photodissociation pathways one-dimensional cuts through the full potential energy surfaces for dissociation into BrO + O as well as Br + O_2 were calculated. Finally, bending potentials are also presented.

Computational Details

All calculations were carried out at the multireference internally contracted configuration interaction (icMRCI) level of theory using the MOLPRO ab initio package.[15]

The MRCI calculations were based on complete active space self-consistent field (CASSCF) orbitals.[16,17] The active space in the CASSCF consisted of the nine orbitals arising from the 2*p* and 4*p* atomic orbitals of oxygen and bromine, respectively (13 active electrons in 9 orbitals). All other low-lying orbitals were fully optimized, but constrained to be doubly occupied.

The calculations of the electronic spectrum, the bending potentials, and the potential curves for dissociation into Br + O_2 were carried out in C_{2v} symmetry, while the treatment of dissociation into BrO + O was in C_s. The size of the resulting CAS was 473 CSFs (configuration state functions) for the B_1 states, 477 CSFs for the A_1 and B_2 states, and 463 CSFs for the A_2 states. In C_s symmetry the corresponding numbers are 954(A′) and 936(A″).

The reference function for the subsequent MRCI calculations employed the active space as in the CASSCF but extended by the doubly occupied two oxygen 2*s* and the bromine 4*s* orbitals. This means all 19 valence electrons were correlated. All single and double excitations with respect to this reference function were included in the MRCI and the doubly external configurations were internally contracted[18,19] (icMRCI). Energy contributions for higher-order excitations have been estimated by the multireference analog[20,21] of the Davidson correction[22] (icMRCI+Q).

For oxygen and bromine, the aug-cc-pVTZ basis sets of Dunning and co-workers[23−25] were employed with omission of the diffuse *f* functions. The total basis set thus obtained is denoted as AVTZ′; it consisted of the following contracted functions: [4*s*3*p*2*d*1*f*] for each oxygen and [6*s*5*p*3*d*1*f*] for bromine with one diffuse *s*, *p*, and *d* function on each atom. To estimate the influence of the basis set flexibility on the excitation energies of OBrO, several other basis sets were applied and are compiled in Table 1.

The electronic ground state of OBrO in C_{2v} symmetry is of $^2B_1$ type and corresponds at its equilibrium geometry to the electronic configuration

$$\text{Core}\ (9a_1)^2\ (5b_2)^2\ (10a_1)^2\ (11a_1)^2\ (6b_2)^2\ (4b_1)^2\ (7b_2)^2\ (2a_2)^2\ (12a_1)^2\ (5b_1)^1$$

or

$$\text{Core}\ (13a')^2\ (14a')^2\ (15a')^2\ (16a')^2\ (17a')^2\ (5a'')^2\ (18a')^2\ (6a'')^2\ (19a')^2\ (7a'')^1$$

in C_s symmetry. It should be mentioned that the ground-state occupation given in the paper of Miller et al.[11] Core···$(14a_1)^2\ (2b_2)^2\ (3a_2)^2\ (7b_1)^1$ appears to be in error. The electronic vertical spectrum of OBrO has been calculated at the experimental equilibrium geometry of Müller et al.[27] (Br−O distance 1.644 Å (3.1067 bohr); ∢OBrO 114.3°).

TABLE 1: Summary of Basis Sets Employed

basis set (abbreviation)	cGTOs[a]	Dunning's notation	comments
VTZ	103	cc-pVTZ[b,d]	
AVTZ	151	aug-cc-pVTZ[b,c,d]	
AVTZ′	130	aug-cc-pVTZ	without diffuse *f* functions
AVTZ′ (ECP)	116	aug-cc-pVTZ	optimized for using in combination with a quasirelativistic effective core potential (ECP)[e] and neglecting the diffuse *f* functions
AVTZ′+*sp*	142	aug-cc-pVTZ	augmented by an additional set of diffuse *s* and *p* functions[f] but without diffuse *f* functions
AVQZ′	205	aug-cc-pVQZ[b,c,d]	without diffuse *f* and *g* functions

[a] Number of basis functions (contracted Gaussian Type Orbitals (cGTOs)). [b] Ref 23. [c] Ref 24. [d] Ref 25. [e] Ref 5. [f] The exponents of the additional set of diffuse *s* and *p* functions were determined in an even-tempered sense as proposed in ref 26: oxygen *s* (0.02419) and *p* (0.01727); bromine *s* (0.01778) and *p* (0.01242).

TABLE 2: Vertical Electronic Excitation Energies ΔE, Transition Dipole Moments $R_{e''e'}$, and Oscillator Strengths *f* of the Lowest-Lying Doublet States of OBrO[a]

state (C_{2v} C_s)	dominant configurations	ΔE (eV)	$R_{e''e'}$ (au)[b,c]	*f*
$1^2B_1/1^2A''$	... $(7b_2)^2\ (2a_2)^2\ (12a_1)^2\ (5b_1)^1$	0.0	-	-
$1^2B_2/1^2A'$	... $(7b_2)^1\ (2a_2)^2\ (12a_1)^2\ (5b_1)^2$	2.43	0.0	0.0
$1^2A_1/2^2A'$	... $(7b_2)^2\ (2a_2)^2\ (12a_1)^1\ (5b_1)^2$	2.51	0.054 (*y*)	0.0
$1^2A_2/2^2A''$	... $(7b_2)^2\ (2a_2)^1\ (12a_1)^2\ (5b_1)^2$	2.69	0.594 (*x*)	0.023
$2^2A_1/3^2A'$	... $(7b_2)^2\ (2a_2)^2\ (12a_1)^2\ (5b_1)^0\ (13a_1)^1$	3.88	−0.047 (*y*)	0.0
$2^2B_2/4^2A'$	... $(7b_2)^2\ (2a_2)^2\ (12a_1)^2\ (5b_1)^0\ (8b_2)^1$	4.51	0.0	0.0
$2^2A_2/3^2A''$	... $(7b_2)^1\ (2a_2)^2\ (12a_1)^2\ (5b_1)^1\ (13a_1)^1$	6.03	0.109 (*x*)	0.002
$2^2B_1/4^2A''$	... $(7b_2)^2\ (2a_2)^2\ (12a_1)^1\ (5b_1)^1\ (13a_1)^1$	6.13	−0.046 (*z*)	0.0

[a] icMRCI+Q results, AVTZ′ basis and experimental (C_{2v}) geometry used (ref 27). [b] In parentheses: polarization of the transition (OBrO is placed in the *xz* plane with *z* being the C_2 axis for C_{2v} symmetry). [c] The $^2B_2 \leftarrow {}^2B_1$ transitions are electric dipole forbidden.

Results and Discussion

The Vertical and Adiabatic Electronic Excitation Energies. As a first step toward discussing photodissociation, it is useful to get an overview of the relevant excited electronic states by calculating the electronic vertical spectrum. This information is especially important for OBrO, because up to now only one excited state has been experimentally investigated, which was characterized by a visible absorption spectrum in the 15500−26000 cm^{-1} (385−645 nm) region with extensive vibronic structure and an intensity maximum at about 20164 cm^{-1} (496 nm).[10−14] Only the three lowest-lying excited states were theoretically studied by Miller et al.[11] and Peterson.[5] We have therefore extended the calculations to include a total of two states for each C_{2v} point group symmetry. Moreover, some preliminary three-state calculations were also carried out.

The calculated vertical excitation energies of doublet states are presented in Table 2, together with the transition dipole moments and oscillator strengths for excitations from the ground

state. From Table 2 it follows that the three lowest-lying vertical excitation energies are obtained close together between 2.4 and 2.7 eV (i.e., 517 and 459 nm), in agreement with the findings of Miller et al.[11] for the corresponding adiabatic transitions, which will be discussed somewhat later in more detail. These three states possess $^2B_2$, $^2A_1$, and $^2A_2$ symmetry and result from excitations of the $7b_2$, $12a_1$, and $2a_2$ orbitals into the singly occupied $5b_1$ orbital.

Another four electronic states are predicted to lie in the energy range up to about 6 eV which is still interesting for atmospheric photochemistry. Those at 3.9 eV (2^2A_1) and 4.5 eV (2^2B_2) are created by excitations from the singly occupied orbital $5b_1$ into the lowest-lying virtual orbitals $13a_1$ and $8b_2$. The last two states (2^2A_2 and 2^2B_1) considered in our two-root calculations show excitation energies around 6 eV. Preliminary three-root calculations predict four further states between 6 and 7 eV (6.0 eV (3^2B_2), 6.4 eV (3^2B_1), 6.5 eV (3^2A_1), and 6.7 eV (3^2A_2)), deriving from $2a_2 \rightarrow 13a_1$, $12a_1 \rightarrow 13a_1$, $11a_1 \rightarrow 5b_1$, and $7b_1 \rightarrow 13a_1$ transitions. The calculated high density of states above 6 eV will make experimental and theoretical investigation of possible photodissociation processes in this energy region much more difficult.

For an assignment of available experimental electronic spectra and for a first impression of those states which could be important for photodissociation we must also look at the electronic transition moments or the oscillator strengths, which are related to the intensities of the transitions from the ground state. Table 2 clearly shows that the most important excited state will be the 1^2A_2 state. This is the only state with a large transition dipole moment (0.594 au), whereas for all other states with exception of the second $^2A_2$ state this quantity is very small (exactly zero for the electric dipole forbidden transitions from the ground state to the $^2B_2$ states). From this it follows that the strongest experimentally observed absorption feature in the UV spectrum of OBrO at about 2.5 eV (496 nm) originates from the 1^2A_2 (C^2A_2) $\leftarrow$ 1^2B_1 (X^2B_1) transition and photodissociation processes in this energy region should start with an excitation to the 1^2A_2 state.

A comparison with calculations of the corresponding chlorine system, OClO, is only possible for the three lowest excitations and shows features similar to OBrO: three close-lying states of $^2B_2$, $^2A_1$, and $^2A_2$ symmetry, but with 0.7 eV to 1 eV higher transition energies ($\approx$3.2 eV (1^2B_2, 1^2A_1) estimated from Figure 5 of ref 28 and 3.66 eV (1^2A_2)[28]).

Before treating larger parts of the potential energy surfaces of OBrO, it is important to estimate the influence of basis set flexibility, especially the role of diffuse functions on the calculated vertical excitation energies. The basis sets considered have been derived from the triple-ζ correlation consistent basis sets of Dunning and co-workers and denoted as VTZ in this paper. Moreover, one basis set of quadruple-ζ quality was used (cf. Table 1). The results of this basis set comparison are compiled in Table 3. For studying the influence of diffuse functions, the VTZ basis was augmented with one set of diffuse *s*, *p*, *d*, and *f* functions (AVTZ). In a somewhat more economical variant, the diffuse *f* functions of the AVTZ basis were neglected (AVTZ′). Comparing the calculated VTZ, AVTZ, and AVTZ′ excitation energies, only minor changes were observed by additional inclusion of diffuse functions (the differences amounted only up to 0.04 eV). This is also true when adding a second set of diffuse *s* and *p* functions (AVTZ′ + *sp*). Therefore all states considered would appear to possess no marked Rydberg character. A further increase of basis set flexibility by changing to a basis set of quadruple-ζ quality (AVQZ′) seems to be not necessary as well, as can be seen from the results of Table 3.

TABLE 3: Vertical Electronic Excitation Energies ΔE[a] for the Doublet States of OBrO. Influence of Basis Set Flexibility and Role of Diffuse Functions

	ΔE (eV)					
	basis set					
	VTZ	AVTZ	AVTZ′	AVTZ′+*sp*	AVQZ′	AVTZ′ (ECP)
state						
1^2B_1	0.0	0.0	0.0	0.0	0.0	0.0
1^2B_2	2.42	2.43	2.43	2.43	2.41	2.39
1^2A_1	2.49	2.51	2.51	2.51	2.49	2.48
1^2A_2	2.68	2.70	2.69	2.69	2.68	2.65
2^2A_1	3.93	3.89	3.88	3.88	3.89	3.81
2^2B_2	4.55	4.51	4.51	4.51	4.52	4.55
2^2A_2	6.05	6.03	6.03	6.02	6.02	5.90
2^2B_1	6.15	6.13	6.13	6.12	6.12	6.01

[a] icMRCI+Q results, experimental geometry used (ref 27).

Summarizing all the basis set investigations we can conclude that the AVTZ′ basis set is a good compromise between basis set quality and economy; therefore it will be used in all subsequent calculations.

Finally, the excitation energies were also calculated using a slightly modified AVTZ′ basis set and a relativistic effective core potential (ECP) for bromine.[5] The AVTZ′(ECP) results presented in Table 3 show that the vertical excitation energies were not significantly affected by this type of ECP approximation; the differences to the AVTZ′ excitation energies are only 0.1 eV at most.

After discussion of the vertical excitation energies we turn now to the adiabatic ones. The following calculations should mainly be considered as a further test of the efficiency and reliability of the method (icMRCI+Q) and basis set (AVTZ′) employed. This test is possible by comparison with the CCSD(T) calculations of Miller et al.[11] (TZ2P basis) and the MRCI study of Peterson[5] with somewhat larger basis sets of quadruple-ζ quality, and moreover by comparison with experimental findings (only for the 1^2B_1 and 1^2A_2 states). As can be seen from Table 4, our theoretical predictions of the geometries and excitation energies of the four lowest-lying states of OBrO are in very close agreement with the previous, above-mentioned theoretical calculations. The differences of the Br−O bond length and OBrO bond angle are at most 0.01 Å and 0.8°, respectively, and in the case of the excitation energies at most 0.06 eV. The differences to the experimental values for the 1^2B_1 and 1^2A_2 states are even smaller. As already pointed out for the vertical excitation energies, there are similarities with the corresponding chlorine system (Table 4, last column). In both systems we observe an extension of the X−O bond length (X = Cl, Br) upon excitation for all three states ($^2B_2$, $^2A_2$, $^2A_1$), whereas the bond angle for the 1^2A_2 state decreases and for the 1^2A_1 state increases slightly. It should be emphasized that the 1^2B_2 state of both OBrO and OClO is an acute-angle state. The differences in the adiabatic excitation energies of the bromine and chlorine systems are found to be in the range 0.4 eV to 0.6 eV, somewhat smaller than those calculated for the vertical excitation energies.

At the end of this section we present some results of the calculation of the low-lying quartet states of OBrO, since excitations from the doublet ground state into quartet states via spin−orbit coupling should be possible.

The first four quartet states were found to lie close together between 5 and 6 eV (Table 5). Photodissociation processes linked to the lowest-lying excited states of OBrO, especially to

TABLE 4: Geometries[a] and Adiabatic Electronic Excitation Energies T_e[b] for the Lowest Bound Doublet States of OBrO. Comparison to OClO

		OBrO (X = Br)			OClO (X = Cl)
state		this work[e] (icMRCI + Q)	KAP[f] (icMRCI + Q)	MNFS[g] CCSD(T)	KAP/PW[h] (icMRCI + Q)
1^2B_1	r(XO)[c]	1.652	1.646	1.660	1.473
	∢(OXO)[c]	114.5	114.7	114.8	117.7
1^2B_2	r(XO)	1.749		1.759	1.597
	∢(OXO)	86.1		85.6	89.7
	T_e	1.58		1.56	1.98
1^2A_2	r(XO)[c]	1.784	1.778	1.785	1.633
	r(OXO)[c]	104.0	104.6	103.2	106.2
	T_e[d]	2.02	2.03	2.08	2.65
1^2A_1	r(XO)	1.768		1.775	1.612
	∢(OXO)	117.3		118.1	120.0
	T_e	2.09		2.03	2.60

[a] Bond lengths in Å, bond angles in degrees. [b] T_e in eV. [c] Experimental values (OBrO): 1.644 Å and 114.3° (1^2B_1) (ref 27) and 1.759 ± 0.010 Å and 104.4 ± 0.5° (1^2A_2) (ref 11). [d] Experimental values: 1.99 eV (OBrO, ref 11), 2.01 eV (OBrO, ref 5), and 2.68 eV (OClO, ref 5). [e] AVTZ′ basis used. [f] Ref 5. [g] Ref 11. [h] Ref 5 for the 1^2B_1 and 1^2A_2 state. Ref 28 for the others.

TABLE 5: Vertical Electronic Excitation Energies ΔE[a] for the Lowest-Lying Quartet States of OBrO[b]

state	dominant configurations	ΔE (eV)
1^4B_2	... $(7b_2)^2$ $(2a_2)^1$ $(12a_1)^2$ $(5b_1)^1$ $(13a_1)^1$	5.09
1^4A_2	... $(7b_2)^1$ $(2a_2)^2$ $(12a_1)^2$ $(5b_1)^1$ $(13a_1)^1$	5.25
1^4B_1	... $(7b_2)^2$ $(2a_2)^2$ $(12a_1)^1$ $(5b_1)^1$ $(13a_1)^1$	5.49
1^4A_1	... $(7b_2)^2$ $(2a_2)^1$ $(12a_1)^2$ $(5b_1)^1$ $(8b_2)^1$	5.97

[a] Related to the 1^2B_1 ground state of OBrO. [b] icMRCI+Q results (AVTZ′ basis), experimental geometry used (ref 27).

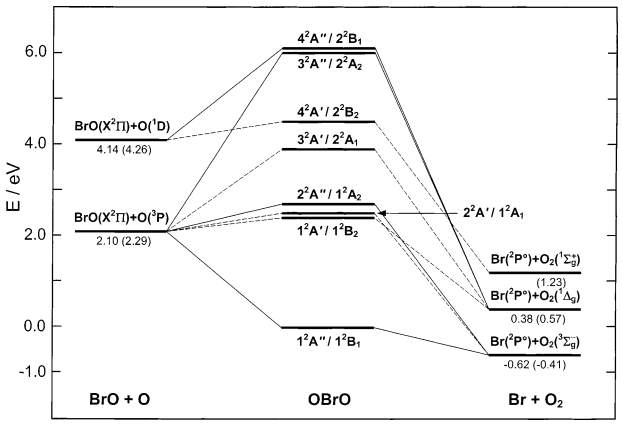

Figure 1. Correlation diagram for the dissociation of OBrO into BrO + O and Br + O_2, assuming C_s symmetry for the BrO + O and C_{2v} symmetry for the Br + O_2 channel. Full lines represent A″ symmetry in C_s, dashed lines correspond to A′ symmetry. The numbers refer to the calculated electronic dissociation energies (without spin−orbit contributions); in parentheses: experimental estimations (cf. Table 6).

the 1^2A_2 state, should not be influenced by quartet states, but for excitation energies larger than 5 eV processes involving quartet states cannot be excluded. Interesting to note, the quartet states of the corresponding chlorine dioxide system were previously calculated to be located at considerably higher energies (6.82 eV ($^4B_2$), 7.96 eV ($^4A_2$), 8.08 eV ($^4A_1$), and 8.27 eV ($^4B_1$)).[28]

Correlation Diagram for Dissociation into BrO + O and Br + O_2. Before starting with actual calculations of some cuts through the potential energy surfaces of OBrO, it is useful for a qualitative understanding of the dissociation processes to draw a correlation diagram for dissociation into both possible channels BrO + O and Br + O_2 (Figure 1).

The vertical excitation energies of OBrO in Figure 1 are taken from Table 2. The (electronic) dissociation energies were calculated in a supermolecule approach and are compared with estimated ("experimental") values obtained from experimental data for heats of formation and experimental excitation energies of the oxygen atom and the oxygen molecule, and corrected for spin−orbit and zero-point energy contributions. Details can be found in Table 6. To the authors' knowledge experimentally determined dissociation energies are not available up to now. The deviations of about 0.2 eV between theoretical predictions and "experimental" findings are expected for this level of theory and basis set.

TABLE 6: Comparison of Calculated Dissociation Energies (supermolecule approach[a]) and Experimental Estimations

	electronic dissociation energies (eV)[b]	
dissociation channel	icMRCI+Q (AVTZ′)	"experimental" estimations[c]
BrO($X^2\Pi$) + O(^3P)	2.10	2.29[d]
BrO($X^2\Pi$) + O(^1D)	4.14	4.26[e]
Br($^2P^o$) + $O_2(^3\Sigma_g^-)$	−0.62	−0.41[f]
Br($^2P^o$) + $O_2(^1\Delta_g)$	0.38	0.57[g]
Br($^2P^o$) + O_2 ($^1\Sigma_g^+$)		1.23[h]

[a] (BrO + O): Br−O_1 10.0 bohr Br−O_2 3.25 bohr (exp. value for BrO[29]) ∢OBrO 114.2° (exp. value for OBrO[27]). (Br + O_2): Br−$O_{1(2)}$ 10.0 bohr O−O 2.30 bohr ($^3\Sigma_g^-$) and 2.32 bohr ($^1\Delta_g$)(exp. values: 2.28 bohr and 2.30 bohr[30]). [b] All values related to the OBrO(1^2B_1) ground state. [c] To make valid comparisons with the theoretical predictions, zero-point vibrational energy (ZPE) and spin−orbit (SO) contributions are removed from the experimental estimates. [d] Estimated by taking the heats of formation $\Delta_f H_0^o$(OBrO: 1.80 eV;[6] BrO: 1.38 eV;[31] O: 2.56 eV[6]) and corrected for ZPE (OBrO: −0.12 eV;[11] BrO: −0.04 eV[30]) as well as SO contributions (BrO: 0.06 eV;[30] O: 0.01 eV[32]). [e] Estimated from the experimental energy difference O(^1D) − O(^3P): 1.97 eV.[32] [f] Estimated by taking the heats of formation $\Delta_f H_0^o$(OBrO: 1.80 eV;[6] Br: 1.22 eV;[6] O_2: 0 eV (standard state)) and corrected for ZPE (OBrO: −0.12 eV;[11] O_2: −0.10 eV[30]) as well as SO contributions (Br: 0.15 eV[32]). [g] Estimated from the experimental energy difference $O_2(^1\Delta_g)$ − $O_2(^3\Sigma_g^-)$: 0.98 eV[30] (T_e). [h] Estimated from the experimental energy difference $O_2(^1\Sigma_g^+)$ − $O_2(^3\Sigma_g^-)$: 1.64 eV[30] (T_e).

In establishing the correlations, we assumed C_s symmetry for the BrO + O dissociation channel and C_{2v} for the Br + O_2 channel; only doublet states of OBrO have been taken into account.

The BrO($X^2\Pi$) ground-state splits into an A′ and an A″ state in C_s symmetry. The interaction with the O(^3P) atom (one A′ and two A″ components in C_s) produces three states of A′ and three of A″ symmetry. First, from Figure 1 it follows that for these six states the $1^2A''(1^2B_1)$ ground state of OBrO and the

three close-lying excited states $1^2A'(1^2B_2)$, $2^2A'(1^2A_1)$, and $2^2A''(1^2A_2)$ are available for correlation. Furthermore, also the $3^2A'(2^2A_1)$ and $3^2A''(2^2A_2)$ states correlate with BrO and O in their ground states. Hence photodissociation processes with excitation energies of about 2.5 eV, which are highly probable because of the large transition dipole moment between the 1^2B_1 ground and 1^2A_2 excited state (Table 2), should produce bromine oxide and the oxygen atom in their electronic ground states.

The interaction of BrO in its ground state with oxygen in its first excited ^1D state gives 10 doublet states, five of A′ and five of A″ symmetry, but only one state of each symmetry ($4^2A'$ (2^2B_2) and $4^2A''$ (2^2B_1)) was calculated in this work. As already mentioned in the last section, besides the 1^2A_2 state only the second $^2A_2$ state possesses a transition moment appreciably larger than zero (Table 2) and therefore also for higher excitation energies of about 6 eV the dissociation products (BrO, O) should be formed exclusively in their ground states.

Consider now the right side of Figure 1, describing the dissociation into Br + O_2. In C_{2v} symmetry the Br($^2P°$) ground-state splits into three components of $^2A_1$, $^2B_1$, and $^2B_2$ symmetry, whereas the ground state of $O_2(X^3\Sigma_g^-)$ becomes a $^3B_1$ state. The interaction of these states of Br and O_2 produces doublet and quartet states of symmetry B_1, A_1, and A_2 each; the doublets correlate with the three lowest 1^2B_1, 1^2A_1, and 1^2A_2 states of OBrO. It is interesting to note from the correlation diagram that the $1^2B_1(1^2A'')$ ground state of OBrO is unstable with respect to dissociation to the ground-state products Br($^2P°$) and $O_2(X^3\Sigma_g^-)$, which lie 0.5 eV below the 1^2B_1 state of OBrO. Because OBrO has been experimentally detected and investigated (cf. the Introduction), a barrier in the dissociation channel must exist to prevent dissociation into Br + O_2 (see also the next section).

The first excited state of O_2 has $^1\Delta_g$ symmetry (splitting into $^1A_1$ and $^1B_1$ in C_{2v}) and couples with Br($^2P°$) to give two A_1, two B_1, one B_2, and one A_2 state, but only four states were calculated in the present work (2^2A_1, 2^2B_1, 1^2B_2, and 2^2A_2) and are shown in Figure 1.

The interaction of Br($^2P°$) with O_2 in its excited $^1\Sigma_g^+$ state leads to three states of the types $^2A_1$, $^2B_1$, and $^2B_2$, but only one of them, the 2^2B_2 state, was considered in our calculations.

Finally, it follows from the correlation diagram in Figure 1 that upon breaking C_{2v} symmetry to C_s the crossing between the 1^2B_2 and the 1^2A_1 states changes to an avoided one, because both become $^2A'$ states. This will certainly influence the dissociation dynamics of OBrO into Br + O_2.

Potential Energy Curves for the BrO + O and Br + O_2 Dissociation Pathways. For a detailed quantitative theoretical description of the dissociation dynamics, complete three-dimensional potential energy surfaces of the relevant electronic states of OBrO are indispensable and calculations along these lines are planned for the near future. However, for the moment, to get a first feeling about the behavior of the excited states of OBrO upon dissociation, some one-dimensional cuts through the global surfaces were calculated.

Figure 2 shows the potential energy curves of the four lowest-lying doublet states of A″ and A′ symmetry, respectively, as functions of one Br−O bond length, keeping the other Br−O distance and the bond angle fixed at the experimental ground-state equilibrium values. Important to note, but not unexpected, the shapes of the curves for the two lowest-lying states of A″ and A′ symmetry upon dissociation are very similar to results obtained previously for OClO by Peterson and Werner (cf. Figure 6 of ref 28). Contrary to the strongly bound ground state (1^2B_1) with a dissociation energy (ΔE_{diss}) of 2.1 eV, the first

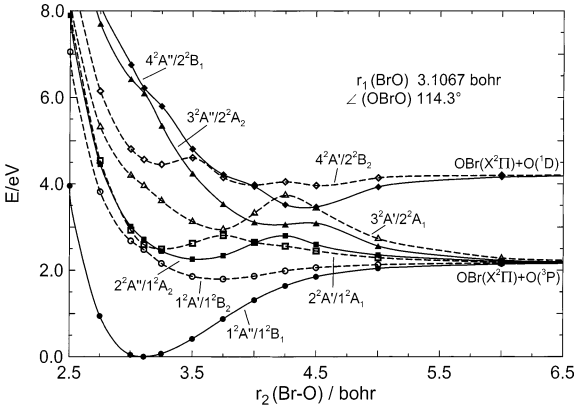

Figure 2. Calculated potential energy curves of the eight lowest-lying doublet states of OBrO for asymmetric dissociation into BrO + O, keeping one Br−O distance and the OBrO bond angle fixed at the experimental ground-state values. Full lines represent states of A″, dashed lines of A′ symmetry.

excited $1^2A'$ (1^2B_2) state is only very weakly bound ($\Delta E_{diss} \approx$ 0.3 eV). In the case of OClO it was found that this state is unbound.[28] The next two close-lying states with $2^2A'$ (1^2A_1) and $2^2A''$ (1^2A_2) symmetries are both weakly repulsive in the outer part and a small barrier of about 0.5 eV appears along the bond stretching coordinate in analogy to the OClO system.[28] The barriers at a Br−O distance of about 3.75 bohr ($2^2A'$) and about 4.25 bohr ($2^2A''$) are the result of avoided crossings with the next higher $3^2A'$ (2^2A_1) and $3^2A''$ (2^2A_2) states, as can be seen in Figure 2. But especially interesting is the fact that in the Franck−Condon region all three states (1^2B_2, 1^2A_1, 1^2A_2) are found close together in the energy range 2.4 eV−2.7 eV and therefore a very complex photodissociation mechanism should be expected. Certainly direct adiabatic dissociation after excitation of the $2^2A''$ (1^2A_2) state is possible, because of the large transition dipole moment calculated for the $2^2A'' \leftarrow 1^2A''$ transition (Table 2), and provided that the excitation energy is large enough ($\Delta E \geq$ 2.8 eV) to overcome the small barrier. Contrary to this, direct adiabatic dissociation through the $1^2A'$ (1^2B_2) and $2^2A'$ (1^2A_1) states is not probable because the $1^2B_2 \leftarrow 1^2B_1$ transition is dipole forbidden and the $1^2A_1 \leftarrow 1^2B_1$ transition possesses only a very small transition moment, as already mentioned in the preceding section.

For the indirect dissociation (predissociation) of the $2^2A''$ (1^2A_2) state in the case of OClO, Peterson and Werner[28] have discussed a three-step mechanism which should also be valid for the bromine system because of the similarity of the potentials. According to this mechanism the $2^2A''$ (1^2A_2) state interacts with the $2^2A'$ (1^2A_1) state via spin−orbit coupling followed by dissociation of the $2^2A'$ (1^2A_1) state and/or by vibronic coupling of the $2^2A'$ (1^2A_1) and $1^2A'$ (1^2B_2) states and fragmentation on the $1^2A'$ (1^2B_2) surface.

The next two well-separated excited states with calculated vertical excitation energies of 3.9 and 4.5 eV have A′ symmetry and dissociate into two different channels producing oxygen in the O(^3P) ground state and in the first excited O(^1D) state, respectively (Figure 2). Both states are more or less strongly repulsive and possess a small barrier along the O−BrO dissociation coordinate. However, these two states should be of minor importance for discussing photodissociation of OBrO because the transition dipole moments for the $2^2A_1 \leftarrow 1^2B_1$ and the $2^2B_2 \leftarrow 1^2B_1$ transitions are very small or zero (Table 2).

Somewhat more interesting are the two close-lying $^2A''$ (2^2A_2, 2^2B_1) states with excitation energies of about 6 eV. Both states are strongly repulsive upon dissociation; they produce, in analogy to the two A′ states discussed before, oxygen in the

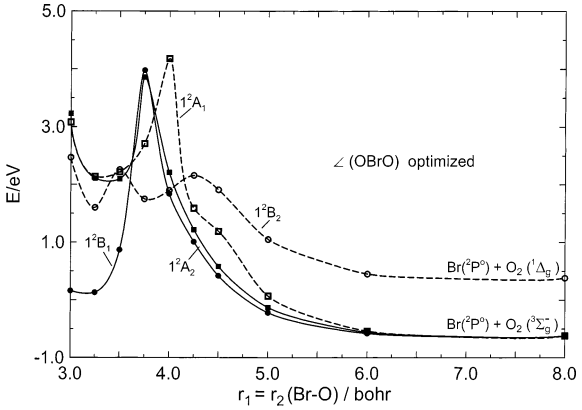

Figure 3. Calculated potential energy curves of the four lowest-lying doublet states of OBrO for symmetric (C_{2v}) dissociation into Br + O_2; the OBrO bond angle was optimized for each calculated Br−O distance. For those states which would become of A″ (A′) type upon breaking C_{2v} symmetry, full (dashed) lines are used.

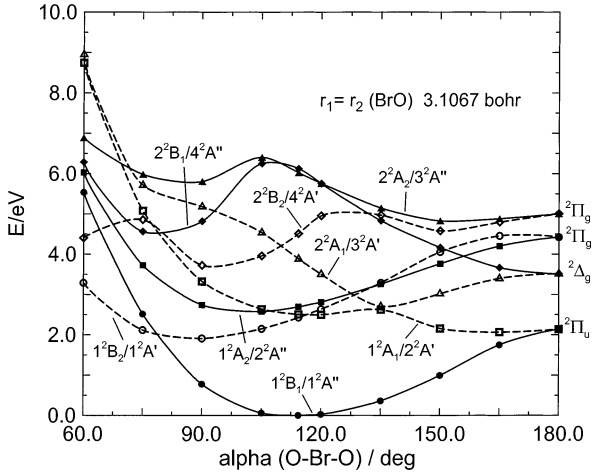

Figure 4. Calculated potential energy curves of the eight lowest-lying doublet states of OBrO as functions of the OBrO bond angle α, keeping both Br−O distances fixed at their experimental ground-state values. Full and dashed lines are used as in Figure 3.

ground state or in the first excited state, respectively, and show nonadiabatic interactions in the Franck−Condon region. But also for these two states the transition moments are very small (Table 2) so that efficient photodissociation for excitation energies of 6 eV should not be observed.

We turn now to the other possible dissociation channel for OBrO leading to Br + O_2 (Figure 3). For these calculations we have assumed a simplified minimum energy path under the constraint of C_{2v} symmetry. The potential energy curves for the four lowest-lying states of OBrO (X^2B_1, 1^2B_2, 1^2A_1, and 1^2A_2) have been computed as functions of the symmetrically stretched Br−O bond lengths; the OBrO bond angle was optimized for each considered Br−O distance.

From Figure 3 it follows that, with exception of the 1^2B_2 state, the other three states studied have relatively large barriers ΔE^B that must be overcome for dissociation leading to Br and O_2 in their ground states (ΔE^B approximately equal to 4.0 eV (1^2B_1), 2.0 eV (1^2A_1), and 1.8 eV (1^2A_2), relative to the respective potential mimimum, corresponding to threshold energies of 4.0, 4.2, and 3.9 eV, respectively, relative to the ground-state minimum. Because of the C_{2v} symmetry constraint the barrier heights are upper limits, but the results of Figure 3 clearly show that the 1^2B_2 state should play a decisive role for the dissociation dynamics of the Br + O_2 channel since the barrier for dissociation is considerably smaller in comparison to those of the states discussed above ($\Delta E^B = 0.7$ eV relative to the 1^2B_2 minimum and 2.3 eV relative to the 1^2B_1 ground-state minimum). For the same reasons as for the BrO + O channel, direct excitation and adiabatic dissociation is improbable, but the 1^2B_2 state should be accessible from initial excitation and predissociation of the 1^2A_2 state.

A further peculiarity of the 1^2B_2 state compared with the other three states investigated is the additional shallow minimum in the dissociation channel (ΔE^B only 0.4 eV relative to this minimum) which could be a symmetric configuration of the isomeric BrOO system, as discussed by Peterson and Werner[4] for the corresponding chlorine system. It can be certainly assumed that this small barrier will not decisively influence the dissociation process.

Figure 3 shows that the dissociation of the 1^2B_2 state produces the oxygen molecule in the first excited state, but it should be emphasized that for asymmetric geometries (C_s symmetry) an avoided crossing between the 1^2A_1 and the 1^2B_2 states takes place late in the exit channel, since both states are then of $^2A'$ symmetry. Therefore it can be expected that the O_2 product is formed not only in the first excited electronic state but also in the ground state.

Finally, it should be mentioned that the findings for OBrO just discussed are in qualitative agreement with results obtained for OClO in a somewhat more detailed two-dimensional treatment.[4] The barriers ΔE^B for OClO are found to be only slightly higher (at the most 0.6 eV) in comparison to the corresponding OBrO system, namely 4.6 eV (X^2B_1), 2.2 eV (1^2A_1), 1.8 eV (1^2A_2), and 1.0 eV (1^2B_2) relative to the respective potential minimum, and threshold energies of 4.6, 4.8, 4.4, and 2.8 eV, respectively, relative to the ground-state minimum.

Potential Energy Curves for the Bending Motion. Besides one-dimensional cuts for describing the dissociation into BrO + O and Br + O_2, it should be useful for a better understanding of the photochemistry of OBrO to probe the angle dependence of all eight states considered (Figure 4).

As can be expected from the results discussed in the last section, the bending potentials in Figure 4, characterized by several curve crossings, give further indication of the rather complicated shapes of the excited-state potential energy surfaces of OBrO, even for the three lowest-lying states with vertical excitation energies around 2.5 eV. Figure 4 shows that the eight states form four Renner-Teller pairs with $^2\Pi_u$, $^2\Delta_g$, $^2\Pi_g$, and again $^2\Pi_g$ symmetry, respectively, at the linear configuration. In analogy to the potential curves for dissociation (cf. the last section), also the bending behavior of the 1^2A_1, 1^2A_2, 1^2B_1, and 1^2B_2 potentials shows a qualitative agreement with the corresponding OClO potentials (cf. Figure 4 of ref 28).

Looking at Figure 4 in more detail, we observe two important crossings in the Franck−Condon region. The first one between the 1^2A_2 and the 1^2A_1 state is even allowed in C_s symmetry and, as discussed by Peterson and Werner for the OClO system,[28] a possible predissociation mechanism of the 1^2A_2 state should be mediated by the interaction of the 1^2A_2 and 1^2A_1 state through spin−orbit coupling. The second crossing between the 1^2B_2 and 1^2A_1 state is changed to an avoided crossing upon C_s distortions, so that in addition to the 1^2A_1 state, also the 1^2B_2 state is possibly involved in the predissociation of the 1^2A_2 state via vibronic coupling. It should be further noted that the 1^2A_1 state has only a very flat minimum in the Franck−Condon region and the linear configuration possesses a lower energy than the bent form. The small barrier between bent and linear

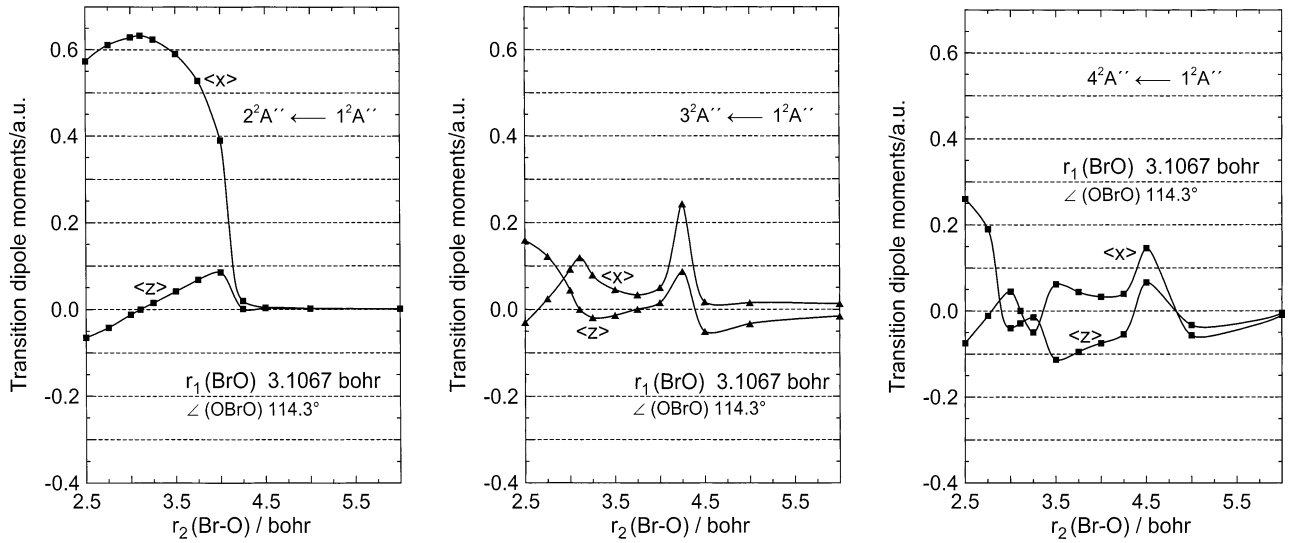

Figure 5. (a)−(c) Calculated transition dipole moments (*x* and *z* components) connecting the three excited $^2A''$ states with the $1^2A''$ ground state as functions of one Br−O bond length, keeping the other Br−O distance and the bond angle fixed at the experimental ground-state values. OBrO is placed in the *xz* plane with the origin of the coordinate system at the center of mass and the axes coinciding with the principal axes of the inertia tensor.

structure is the result of an avoided crossing of the 1^2A_1 and 2^2A_1 states at an OBrO angle of about 135°.

Two further crossings in C_{2v}, which become avoided ones in C_s symmetry, are observed between the 1^2B_2 and 2^2A_1 states at about 127° and between the 2^2A_1 and 2^2B_2 states at a bond angle of about 110°.

Finally it should be mentioned that the higher-lying states (2^2B_1, 2^2A_2, and 2^2B_2) possess two minima in the bending coordinate, with exception of the 2^2A_1 state ($\sphericalangle$ OBrO ∼ 135°).

These minima are found at very small angles on one hand and at angles at or near the linear configuration on the other. The barriers between the two minima are probably the result of avoided crossings with higher-lying states, not calculated in this work.

Geometry Dependence of the Transition Dipole Moments. For a quantitative theoretical description of photodissociation dynamics besides the relevant potential energy surfaces, also the transition dipole moments, connecting the ground and excited states have to be calculated as functions of the nuclear (internal) coordinates. Therefore these quantities will be shortly discussed in the following, taking into account that for excitations from the vibrational ground state the transition dipole moment functions near to the Franck−Condon region play the decisive role.

In Figures 5a−c, the transition dipole moments connecting the three calculated excited $^2A''$ states with the $1^2A''$ ground state are presented as functions of one Br−O bond length. The corresponding values for the excited states of $^2A'$ symmetry remain very small or zero under oxygen atom abstraction as already found for the vertical transitions in the equilibrium ground-state geometry (Table 2). This implies that direct photoinduced dissociation of these states is very improbable.

Figures 5a−c show a completely different behavior of the transition dipole moment functions for transitions to the $2^2A''$ state on one hand and to the $3^2A''$ and $4^2A''$ states, respectively, on the other.

The *x* component of the transition dipole moment to the $2^2A''$ state (Figure 5a) is large in the Franck−Condon region (about 0.6 au), emphasizing the importance of this state for photodissociation processes of OBrO. At larger Br−O distances, we observe a steep decrease to zero. The *z* component is zero for the symmetric C_{2v} geometry, remains considerably smaller than $\langle x \rangle$ and also approaches zero for larger distances.

Contrary to this, both components of the transition dipole moments to the next two higher-lying $^2A''$ states are very small in the Franck−Condon region and become zero for bromine atom abstraction (Figures 5b and 5c). Therefore, direct photodissociation through these states should not be very probable, as already found for the states with A′ symmetry. The variations of the transition dipole moments at a Br−O distance of about 3 au and especially in the range of 4.0−4.75 au are caused by avoided crossings taking place in these regions (cf. Figure 2).

Conclusions

The results and discussions presented in the preceding sections show that for photodissociation processes of bromine dioxide a rather complex behavior is to be expected. The density of states and the resulting coupling of electronic terms in the energy range up to 6 eV will make OBrO interesting for atmospheric photochemistry. Furthermore, the findings of our study demonstrate the expected similarity to the corresponding chlorine system.

Efficient (direct) photodissociation into BrO + O should take place after excitation of the $1^2A_2/2^2A''$ state at an excitation energy of 2.7 eV because of the large transition dipole moment calculated for the $2^2A''/1^2A_2 \leftarrow 1^2A''/1^2B_1$ transition. But it should be mentioned that for the elucidation of the role of the small barrier in the dissociation channel of the $2^2A''$ state, a three-dimensional treatment − calculation of the complete potential energy surface − is necessary. Important to note is that in analogy to the OClO system in the Franck−Condon region, two further states ($1^2B_2/1^2A'$ and $1^2A_1/2^2A'$) are predicted close to the $1^2A_2/2^2A''$ state. Though both states possess only small (or zero) transition dipole moments to the ground state, predissociation should be possible via nonadiabatic interactions with the $2^2A''$ state. Clearly this complex situation at excitation energies around 2.5 eV makes a realistic theoretical description of the photodissociation dynamics of OBrO rather difficult.

The next two states at 3.9 eV ($2^2A_1/3^2A'$) and 4.5 eV ($2^2B_2/4^2A'$) are well-separated from lower- and higher-lying states, but they should be of minor importance for OBrO photodisso-

ciation because of their very small transition dipole moments to the ground state. Further, our calculations predict two close-lying excited $^2A''$ states at about 6 eV. Both states are strongly repulsive upon dissociation into BrO + O producing oxygen in the ground or the first excited state and should exhibit nonadiabatic interactions in the Franck−Condon region.

Concerning dissociation into Br + O_2, the similarity to the corresponding OClO system is also evident. The calculations were carried out only for the four lowest-lying states (1^2B_1, 1^2B_2, 1^2A_1, and 1^2A_2) under the constraint of a simplified minimum energy path assuming C_{2v} symmetry. Because of the large barriers which must be overcome for dissociation into Br + O_2 for the 1^2B_1, 1^2A_1, and 1^2A_2 states (4.0, 2.0, and 1.8 eV relative to the respective potential minimum), only the 1^2B_2 state with a considerably lower barrier of 0.7 eV should play a decisive role for the Br + O_2 channel. However the $1^2B_2 \leftarrow 1^2B_1$ transitions are dipole forbidden so that direct excitation and dissociation of the 1^2B_2 state should be improbable; but, as already discussed for the BrO + O channel, indirect dissociation after excitation of the 1^2A_2 state is conceivable.

For the intended extension of our investigations toward a treatment of the OBrO photodissociation dynamics, complete three-dimensional potential energy surfaces for the $1^2A''$ ground state and the most important $2^2A''$ excited state are to be calculated; moreover the couplings with close-lying excited states must be included. Work in this direction is under way.

References and Notes

(1) Wayne, R. P.; Poulet, G.; Biggs, P.; Burrows, J. P.; Cox, R. A.; Crutzen, P. J.; Hayman, G. D.; Jenkin, M. E.; Le Bras, G.; Moortgat, G. K.; Platt, U.; Schindler, R. N. *Atmos. Environ.* **1995**, *29*, 2677.

(2) Sander, S. P.; Friedl, R. R.; Francisco, J. S. In *Progress and Problems in Atmospheric Chemistry*; Barker, J. R. Ed.; World Scientific: Singapore, 1995; p 876.

(3) Vaida, V.; Simon, J. D. *Science* **1995**, *268*, 1443.

(4) Peterson, K. A.; Werner, H.-J. *J. Chem. Phys.* **1996**, *105*, 9823, and references therein.

(5) Peterson, K. A. *J. Chem. Phys.* **1998**, *109*, 8864, and references therein.

(6) Klemm, R. B.; Thorn, R. P., Jr.; Stief, L. J.; Buckley, Th. J.; Johnson, R. D., III. *J. Phys. Chem. A* **2001**, *105*, 1638, and references therein.

(7) (a) Renard, J.-B.; Pirre; M.; Robert, C.; Huguenin, D. *J. Geophys. Res.* **1998**, *103*, 25383. (b) Berthet, G.; Renard, J.-B.; Chartier, M.; Pirre, M.; Robert, C. *J. Geophys. Res.* Accepted for publication (private communication by J.-B. Renard).

(8) Chipperfield, M. P.; Glassup, T.; Pundt, I.; Rattigan, O. V. *Geophys. Res. Lett.* **1998**, *25*, 3575.

(9) Erle, F.; Platt, U.; Pfeilsticker, K. *Geophys. Res. Lett.* **2000**, *27*, 2217.

(10) Rattigan, O. V.; Jones, R. L.; Cox, R. A. *Chem. Phys. Lett.* **1994**, *230*, 121.

(11) Miller, C. E.; Nickolaisen, S. L.; Francisco, J. S.; Sander, S. P. *J. Chem. Phys.* **1997**, *107*, 2300.

(12) Kölm, J.; Engdahl, A.; Schrems, O.; Nelander, B. *Chem. Phys.* **1997**, *214*, 313.

(13) Lee, Y.-C.; Lee, Y.-P. *J. Phys. Chem. A* **2000**, *104*, 6951.

(14) Knight, G.; Ravishankara, A. R.; Burkholder, J. B. *J. Phys. Chem. A* **2000**, *104*, 11121.

(15) *MOLPRO (Version 96.4)* is a package of ab initio programs written by H.-J. Werner and P. J. Knowles with contributions of J. Almlöf, R. D. Amos, A. Berning, M. J. O. Deegan, F. Eckert, S. T. Elbert, C. Hampel, R. Lindh, W. Meyer, A. Nicklass, K. Peterson, R. Pitzer, A. J. Stone, P. R. Taylor, M. E. Mura, P. Pulay, M. Schuetz, H. Stoll, T. Thorsteinsson, and D. L. Cooper.

(16) Werner, H.-J.; Knowles, P. J. *J. Chem. Phys.* **1985**, *82*, 5053.

(17) Knowles, P. J.; Werner, H.-J. *Chem. Phys. Lett.* **1985**, *115*, 259.

(18) Werner, H.-J.; Knowles, P. J. *J. Chem. Phys*. **1988**, *89*, 5803.

(19) Knowles, P. J.; Werner, H.-J. *Chem. Phys. Lett.* **1988**, *145*, 514.

(20) Blomberg, M. R. A.; Siegbahn, P. E. M. *J. Chem. Phys.* **1983**, *78*, 5682.

(21) Simons, J. *J. Phys. Chem.* **1989**, *93*, 626.

(22) Langhoff, S. R.; Davidson, E. R. *Int. J. Quantum Chem.* **1974**, *8*, 61.

(23) Dunning, T. H., Jr. *J. Chem. Phys.* **1989**, *90*, 1007.

(24) Kendall, R. A.; Dunning, T. H., Jr.; Harrison, R. J. *J. Chem. Phys.* **1992**, *96*, 6796.

(25) Wilson, A. K.; Woon, D. E.; Peterson, K. A.; Dunning, T. H., Jr. *J. Chem. Phys.* **1999**, *110*, 7667.

(26) Lee, T. J.; Schaefer, H. F., III. *J. Chem. Phys.* **1985**, *83*, 1784.

(27) Müller, H. S. P.; Miller, C. E.; Cohen, E. A. *J. Chem. Phys.* **1997**, *107*, 8292.

(28) Peterson, K. A.; Werner, H.-J. *J. Chem. Phys.* **1992**, *96*, 8948.

(29) Alcami, M.; Cooper, I. L. *J. Chem. Phys.* **1998**, *108*, 9414.

(30) Huber, K. P.; Herzberg, G. *Molecular Spectra and Molecular Structure*, *IV. Constants of Diatomic Molecules*; Von Nostrand Reinhold: New York, 1979.

(31) Chase, M. W. *J. Phys. Chem. Ref. Data* **1996**, *25*, 1069.

(32) Moore, C. E. *Atomic Energy Levels*, NSRDS-NBS 35, Office of Standard Reference Data, National Bureau of Standards, Washington, DC, 1971.